PARAMETRIC ANALYSIS OF FORCES AND STRESS IN SUPERCONDUCTING MAGNETS

P. Fessia, F. Regis, E. Todesco
Magnets, Superconductors , and Cryostats (MSC)
Technology Department (TE)

CONTENTS

- Aim of the work
- Forces and Stress in Quadrupoles
  - Analytical formulae for e.m. forces and comparison with FEM models
  - Analytical formulae for mechanical stress and comparison with FEM models
  - E.m. forces and mechanical stress at short sample
  - Iron effect
  - Comparison with real cross sections
  - Conclusions
- Forces and Stress in Dipoles
  - …

CONTENTS

- Aim of the work
- Forces and Stress in Quadrupoles
  - Analytical formulae for e.m. forces and comparison with FEM models
  - Analytical formulae for mechanical stress and comparison with FEM models
  - E.m. forces and mechanical stress at short sample
  - Iron effect
  - Comparison with real cross sections
  - Conclusions
- Forces and Stress in Dipoles
  - …

Aim of the work

- In superconducting magnets, large electro-magnetic (e.m.) forces and related stress are generated by the interaction of the transport current with the magnetic field.
- Mechanical stress shall be limited to avoid superconductor degradation phenomena and insulation creep.
- The Nb_3Sn is considered the most suitable superconductor for new generation superconducting accelerator magnets (peak fields > 10 T). The s.c. properties of Nb_3Sn are strongly dependent on the mechanical stress applied.
- **We aim at provide simple analytical tools to estimate the e.m. forces and mechanical stress in a superconducting coil as a function of the aperture radius r_i, coil equivalent width w, and superconductor type (Nb-Ti, Nb_3Sn).**

CONTENTS

- Aim of the work
- Forces and Stress in Quadrupoles
  - Analytical formulae for e.m. forces and comparison with FEM models
  - Analytical formulae for mechanical stress and comparison with FEM models
  - E.m. forces and mechanical stress at short sample
  - Iron effect
  - Comparison with real cross sections
  - Conclusions
- Forces and Stress in Dipoles
  - …

Quadrupoles – Coil Models

Analytical coil model

- Sector coil layout at 30 (cancel the sixth order field harmonic)
- Constant current density $j(r)=j$
- Aperture radius r_i
- Coil equivalent width w

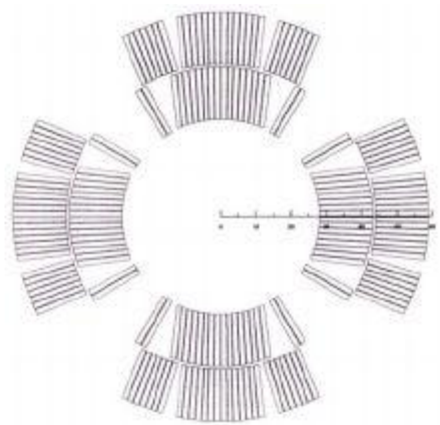

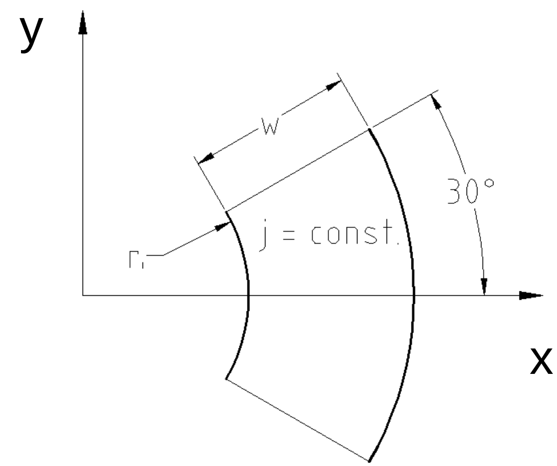

FEM coil model

- 2D FEM model - ANSYS™
- Coupled analysis: magnetic-mechanical
- Magnetic analysis solves for the Magnetic Vector Potential (A_z component)
- Mechanical symmetry constraints on coil mid-plain
- Infinitely rigid collar (radial mech. constraints)

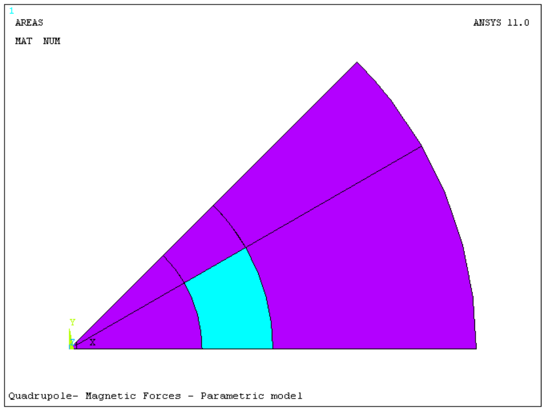

Quadrupoles – Analytical Model Validation

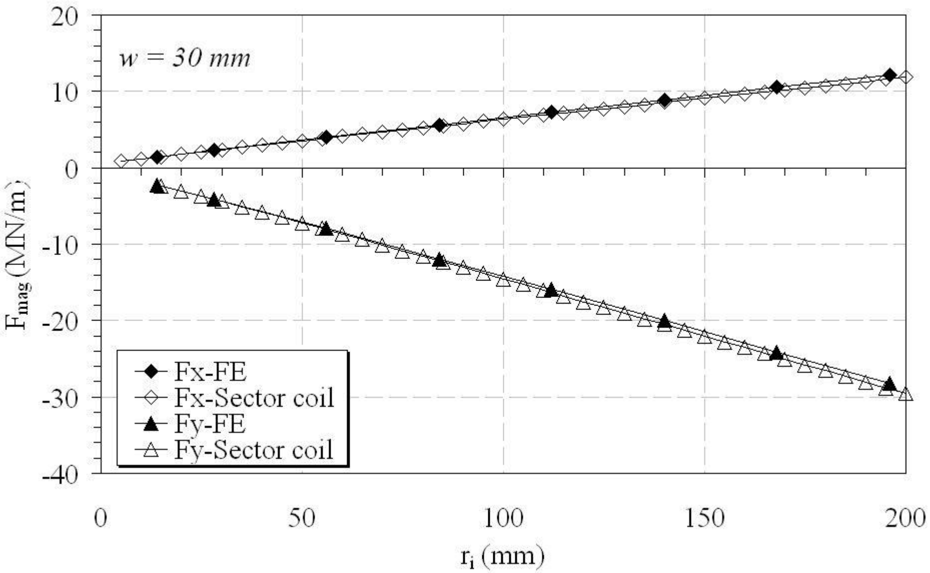

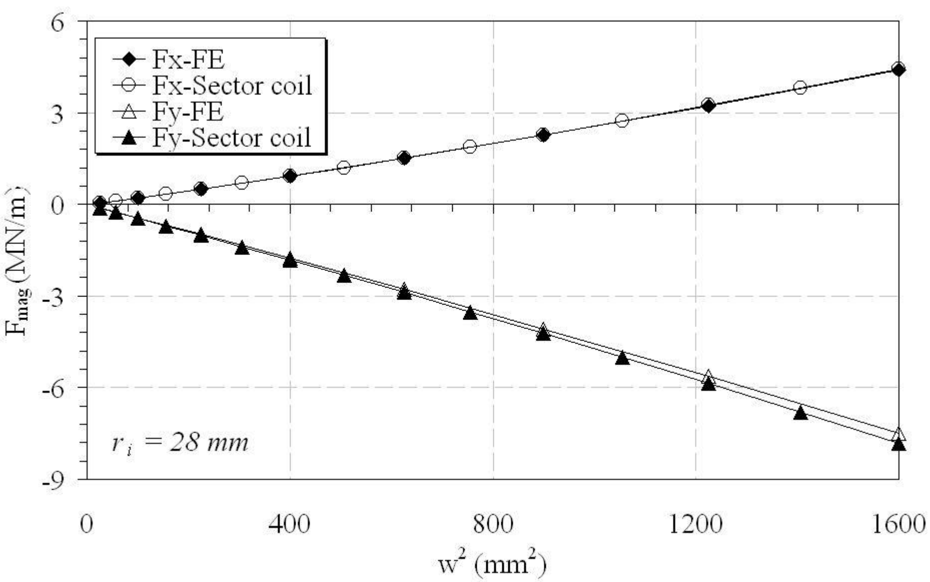

- Parametric analysis carried out on:
  1. r_i : [14,28,56,84,112,140,168,196] mm
  2. w: [5,10,15, 20,25, 30,35,40] mm
- j=1000 A/mm^2 regardless of the layout

- Good agreement for the field in the aperture (G), worst inside the coil
- On the other hand the magnetic energy and the magnetic forces are in good agreement with numerical results

- F_{mag} follow a linear trend with: r_i and w^2
- F_x underestimates the numerical value of about 4%
- F_y overestimates the numerical value of <3%

QUADRUPOLES – ANALYTICAL MODEL VALIDATION

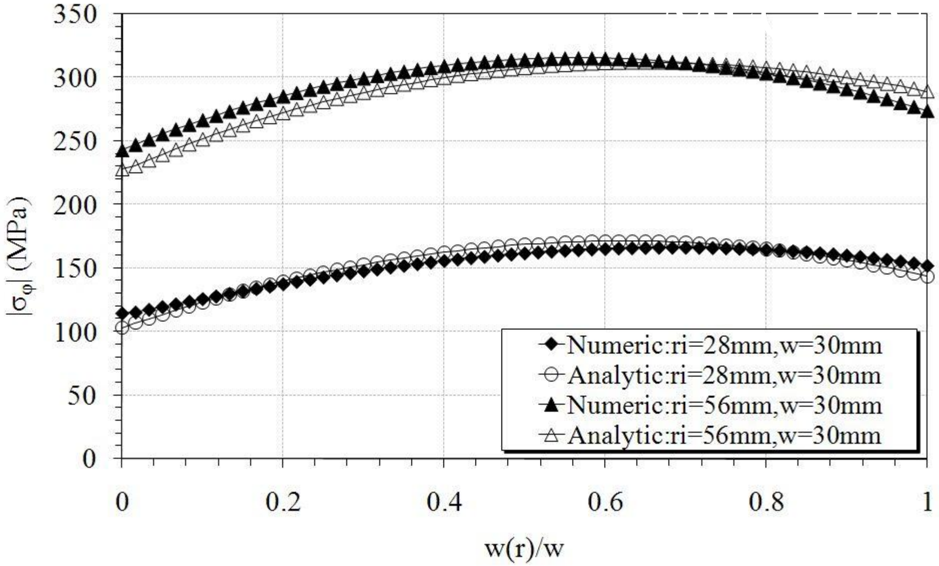

Azimuthal stress

$$\sigma_\varphi(r) = -\frac{j^2 \mu_0 \sqrt{3}}{16\pi r^2}\left[r^4 - r_i^4 + 4r^4 \ln\left(\frac{r_i + w}{r}\right)\right]$$

- $\sigma_{\varphi,max}$ overestimates the numerical value of about 5%.
- For thin coils and large apertures, the peak stress position agreement is within 10%.

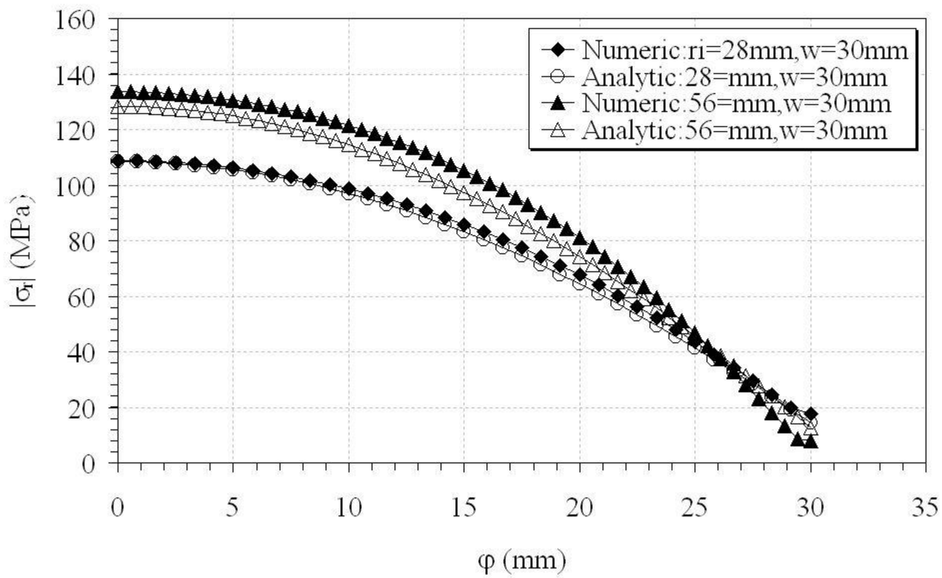

Radial stress

$$\sigma_r(\varphi) = -\frac{j^2 \mu_0 \sin(2\alpha_0)}{36\pi (r_i + w)^2} f_{pr}(r_i^4, w^4, \varphi)$$

- $\sigma_{r,max}$ along the mid-plane (φ=0).
- The peak radial stress overestimation is ~10% for large r_i and thin coils.

Quadrupoles – Anisotropy Analysis

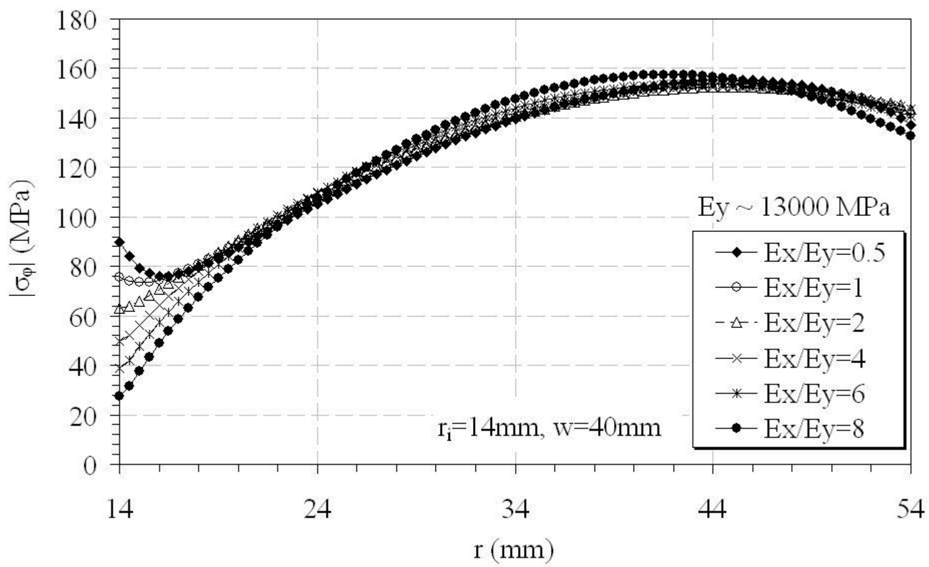

- The shear effect is not taken into account → no quantification of the material effect (Young's modulus *E*)
- Superconductor cables are anisotropic
- **Effect of anisotropy ratio E_r/E_φ has been numerically evaluated**

E_r/E_φ = [0.5,1,2,4,6,8] with $E_{\varphi,ref}$ =13 GPa (LHC-MB outer layer)

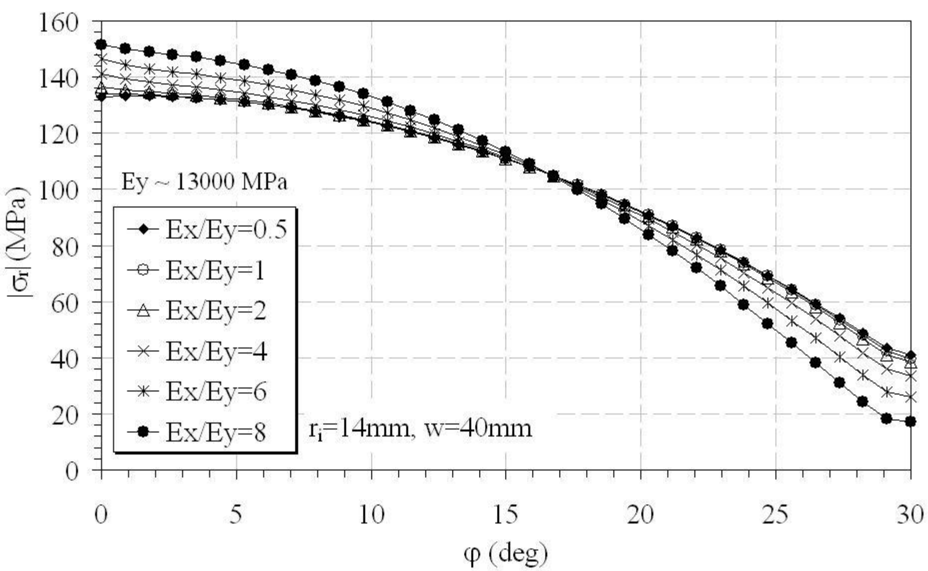

- $|\sigma_{\varphi,max}|$ agreement <2.5%
- $r(\sigma_{\varphi,max})$ agreement <10%
- Larger errors at the inner radius, where the impact on superconductor performance is second order

No considerable difference in peak stress due to anisotropic coil, compared to the isotropic case

CONTENTS

- Aim of the work
- Forces and Stress in Quadrupoles
  - Analytical formulae for e.m. forces and comparison with FEM models
  - Analytical formulae for mechanical stress and comparison with FEM models
  - E.m. forces and mechanical stress at short sample
  - Iron effect
  - Comparison with real cross sections
  - Conclusions
- Forces and Stress in Dipoles
  - …

CRITICAL SURFACE PARAMETERIZATION

Nb-Ti

$$j_{c,Nb-Ti} = \frac{\kappa c B^*_{c2}}{1+\kappa c r_i \lambda(r_i, w)\gamma_0 \ln\left(1+\frac{w}{r_i}\right)}$$

Nb_3Sn

$$j_{c,Nb_3Sn} = \frac{\kappa c}{2}\left(\sqrt{\frac{4B^*_{c2}}{\kappa c \lambda \gamma}+1}-1\right)$$

- κ: cable dilution factor, ranging in [0.23-0.35] (LHC-MQ: κ =0.25)
- B_{c2}: critical field (T)
- c: critical surface slope (A/Tm^2)
- $\lambda = B_p/(G_c r_i)$ (adim)
- $\gamma = \ln(1+w/r_i)\gamma_0 = \ln(1+w/r_i)$ 0.693e-6 (30 layout) (Tm^2/A)

Field gradient $G = j\gamma$

Peak field $B_p = j\lambda(r_i, w)\gamma$

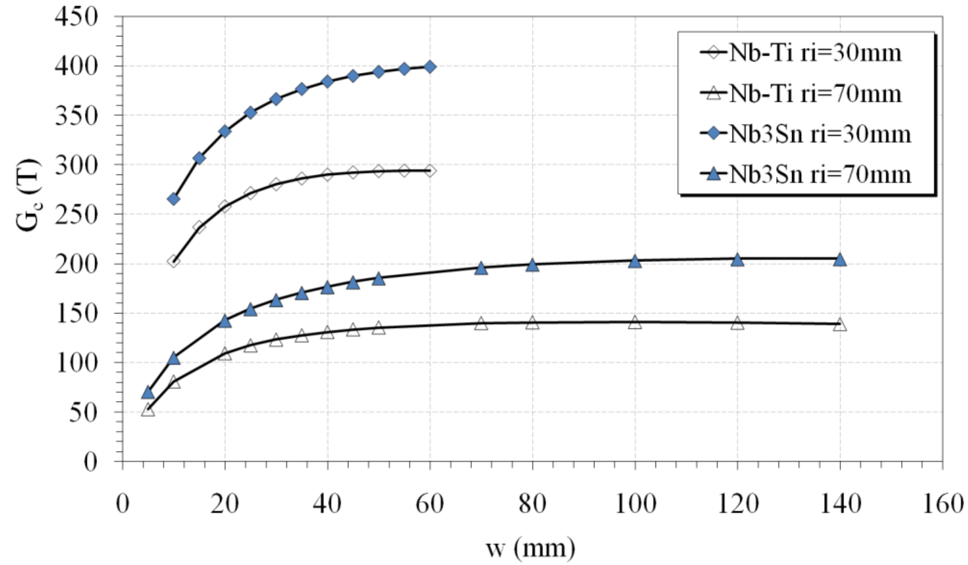

	Nb-Ti		Nb_3Sn	
T (K)	1.9	4.2	1.9	4.2
c (A/Tm^2)	6e8	6e8	4e9	3.9e9
B_{c2} (T)	13	10	23.1	21

L. Rossi, E. Todesco, “Electromagnetic design of superconducting quadrupoles”, Phys. Rev. 9, 102401 (2006)

Quadrupoles – forces at short sample

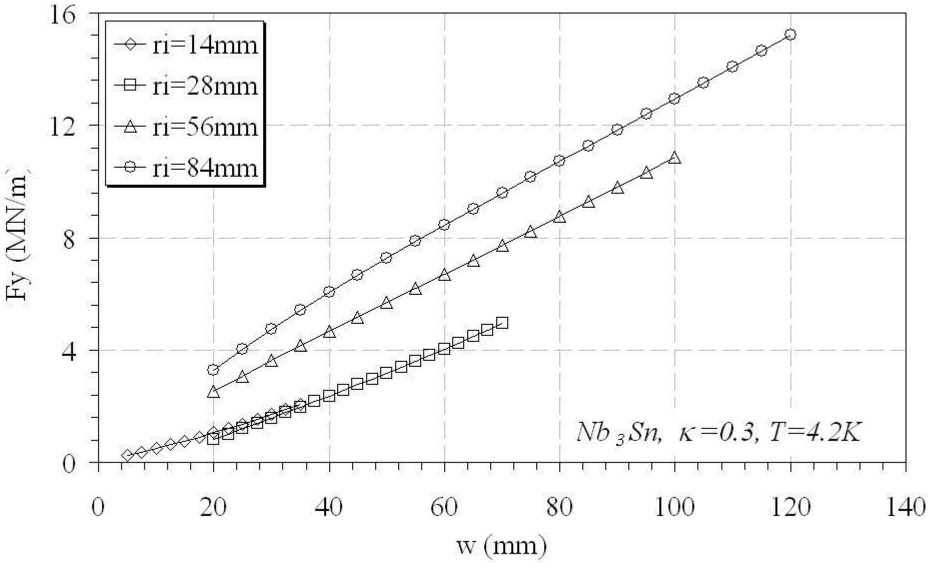

Model input

- κ set to 0.3 in order to have comparable results
- r_i ranges in [14-84] mm
- w ranges in [5-$w(G_{sat})$] mm

- F_{mag} proportional to j^2
- F_{mag} almost linear with the increased width
- Increase in net force F_{mag} is proportional to the ratio of critical current between two superconductors:

$$F_{Nb_3Sn} = \left(\frac{j_{Nb_3Sn}}{j_{Nb-Ti}} \right)^2 F_{Nb-Ti}$$

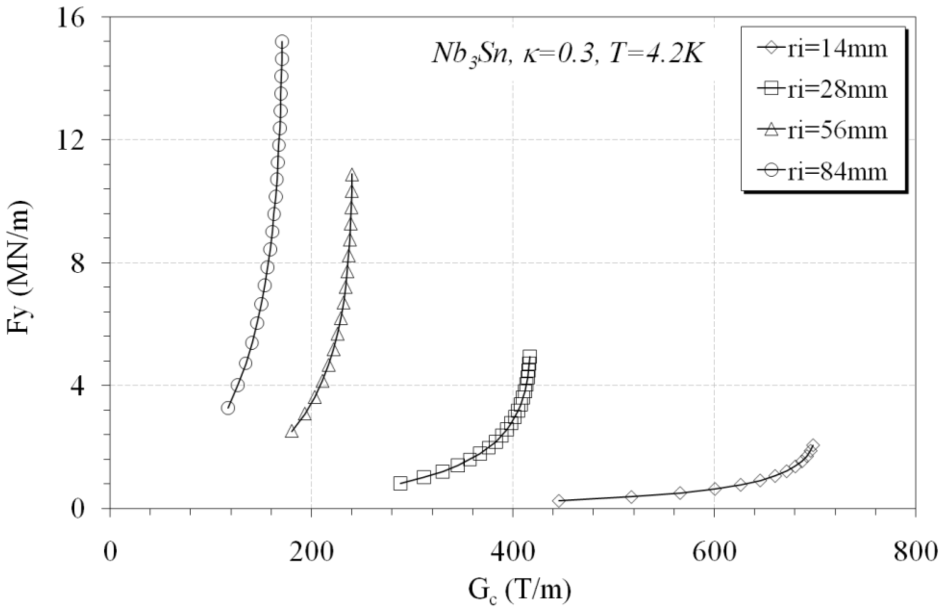

Quadrupoles – $\sigma_{\varphi,max}$ at short sample

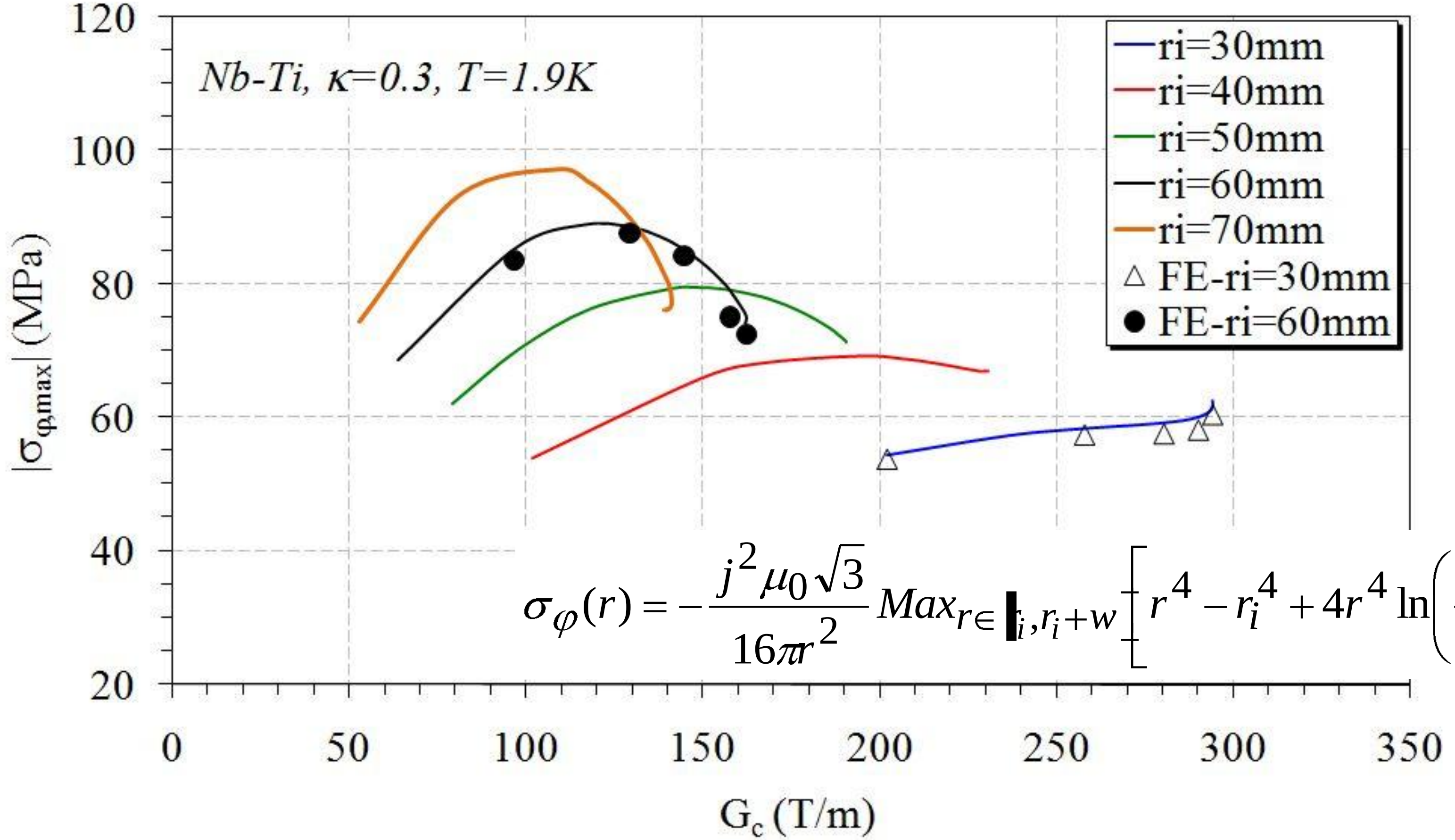

$$\sigma_{\varphi}(r) = -\frac{j^2 \mu_0 \sqrt{3}}{16\pi r^2} Max_{r\in[r_i, r_i+w]}\left[r^4 - r_i^4 + 4r^4 \ln\left(\frac{r_i+w}{r}\right)\right]$$

- $r(\sigma_{\varphi,max})$ obtained from the solution of an implicit equation
- The $\sigma_{\varphi,max}$–G_c curve shows a local maximum, depending on the aperture r_i, coil width w and dilution factor κ.

QUADRUPOLES – $\sigma_{\varphi,max}$ AT SHORT SAMPLE

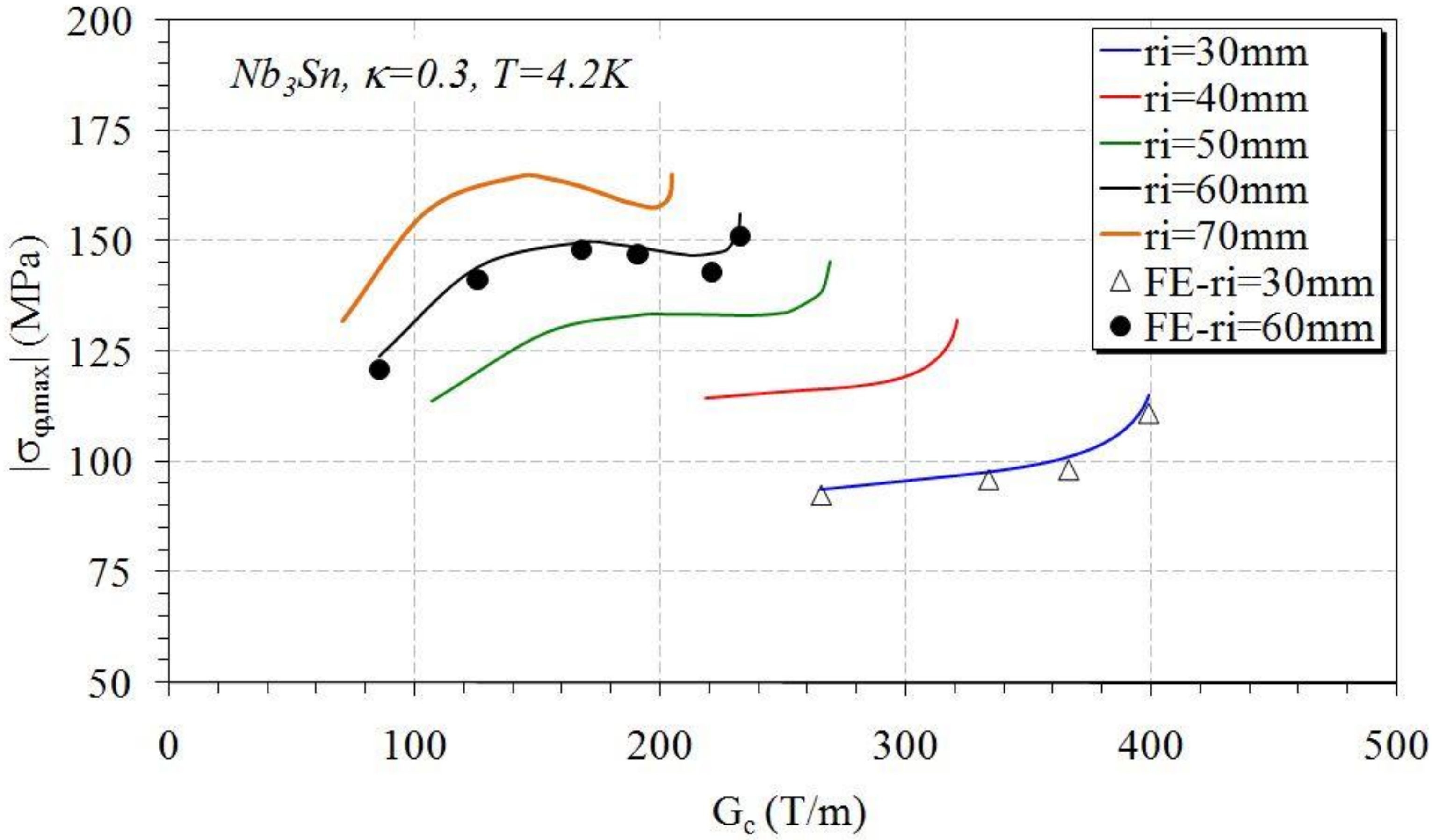

- For aperture radii >60mm, the peak stress is close to the mechanical limit before superconductor degradation. This value is assumed to be about 150-200 MPa.

Quadrupoles – $\sigma_{\varphi,max}$ at short sample

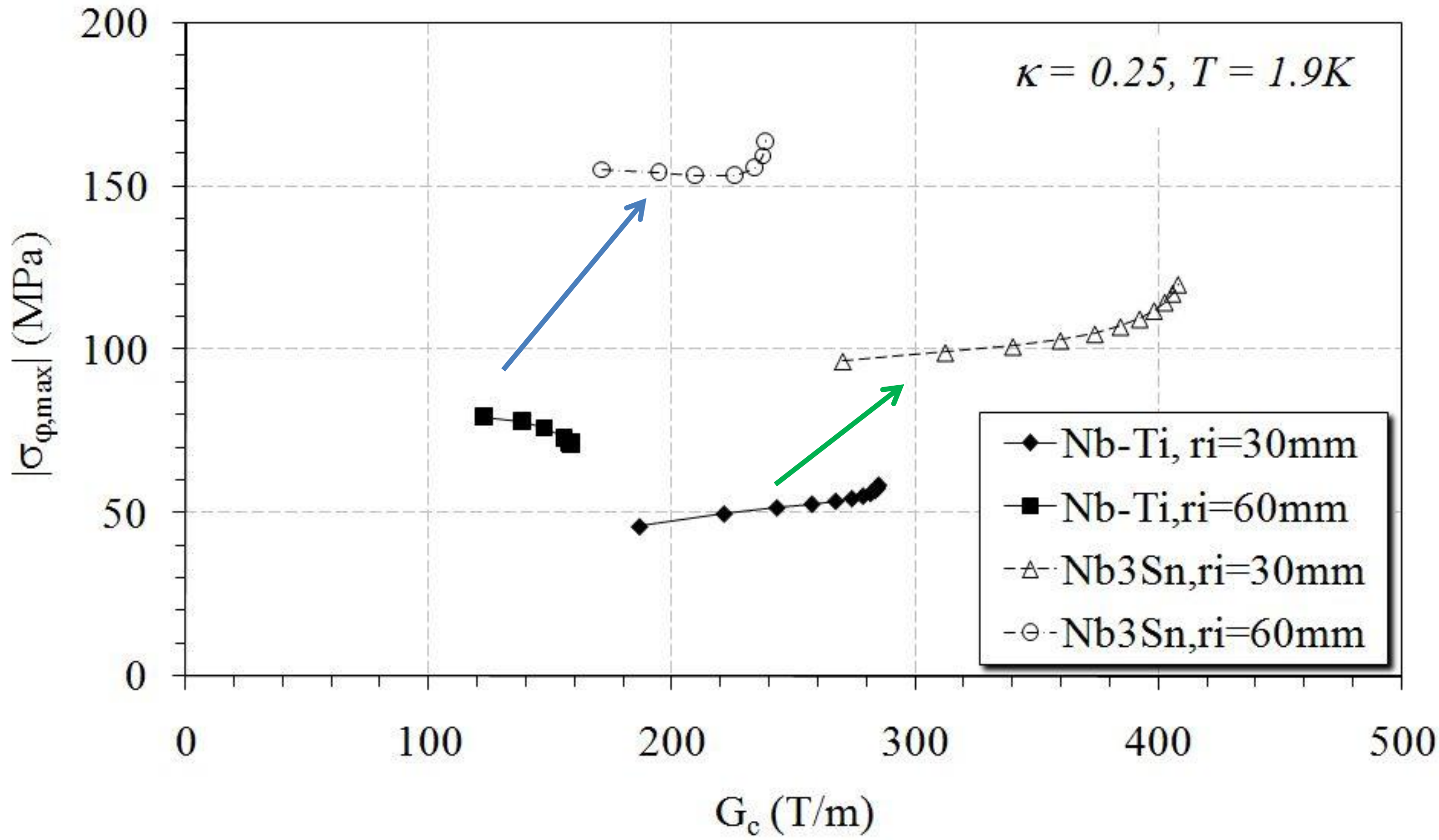

- T=1.9 K, $j_{c,Nb3Sn}/j_{c,Nb\text{-}Ti}$=1.4 → $\sigma_{\varphi,max}$ doubles
- G_c=280 T/m (r_i=30 mm): $w_{Nb\text{-}Ti}$ = 40 mm (1.9K), w_{Nb3Sn}=14 mm (4.2K)

CONTENTS

- Aim of the work
- Forces and Stress in Quadrupoles
  - Analytical formulae for e.m. forces and comparison with FEM models
  - Analytical formulae for mechanical stress and comparison with FEM models
  - E.m. forces and mechanical stress at short sample
  - Iron effect
  - Comparison with real cross sections
  - Conclusions
- Forces and Stress in Dipoles
  - …

Quadrupoles – Iron Effect

- Using an iron yoke we increase the field gradient ΔG and the peak field ΔB_p for a given j.
- <u>The expression of j has to be revised</u>
- No iron saturation ($\mu_r \rightarrow \infty$)
- G_c and B_p considered as linear functions of j

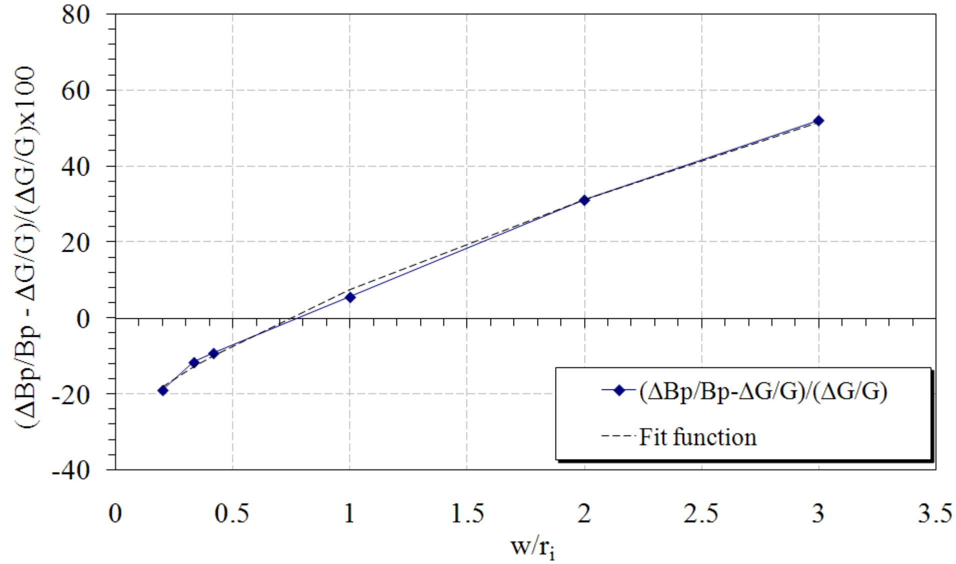

- The iron effect has been analytically accounted for using the *Image Current* approach
- Collar width: $w_{coll} = R_{yoke} - r_o$
- w_{coll} ranges in [10-50] mm
- G_c analytically derived
- B_p numerically evaluated

Empirical fit

$$\frac{\Delta B_p}{B_p} - \frac{\Delta G}{G} = \frac{\Delta G}{G}\left[p_0 + p_1\left(\frac{w}{r_i}\right)^q\right]$$

With:

- p_0=0.3
- p_1=0.374
- q=0.861

$\gamma_{iron} \rightarrow j_{iron}$

Quadrupoles – iron effect

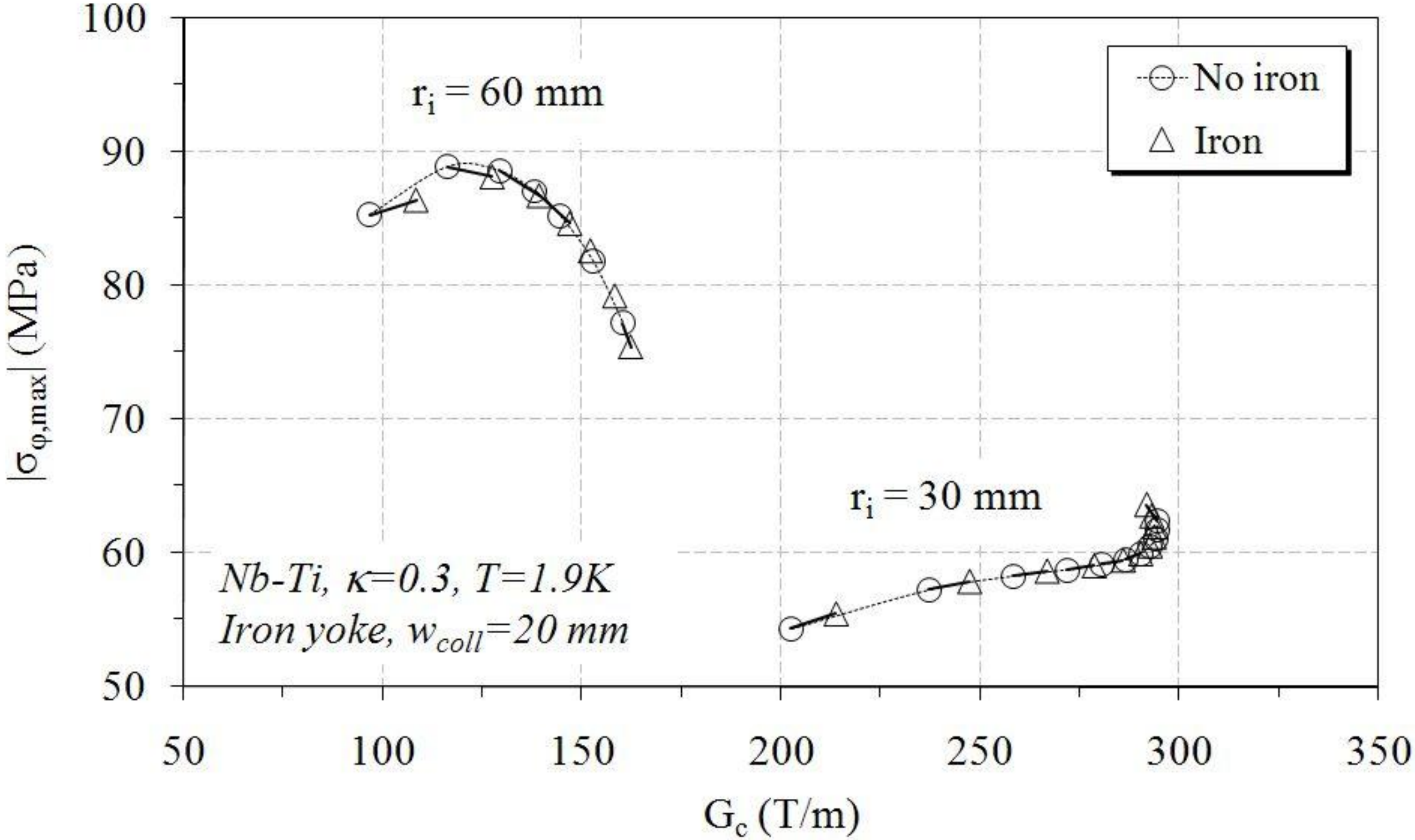

- $\sigma_{\varphi,max}$ for iron (w_{coll}=20 mm) and ironless case are compared

Quadrupoles – Iron Effect

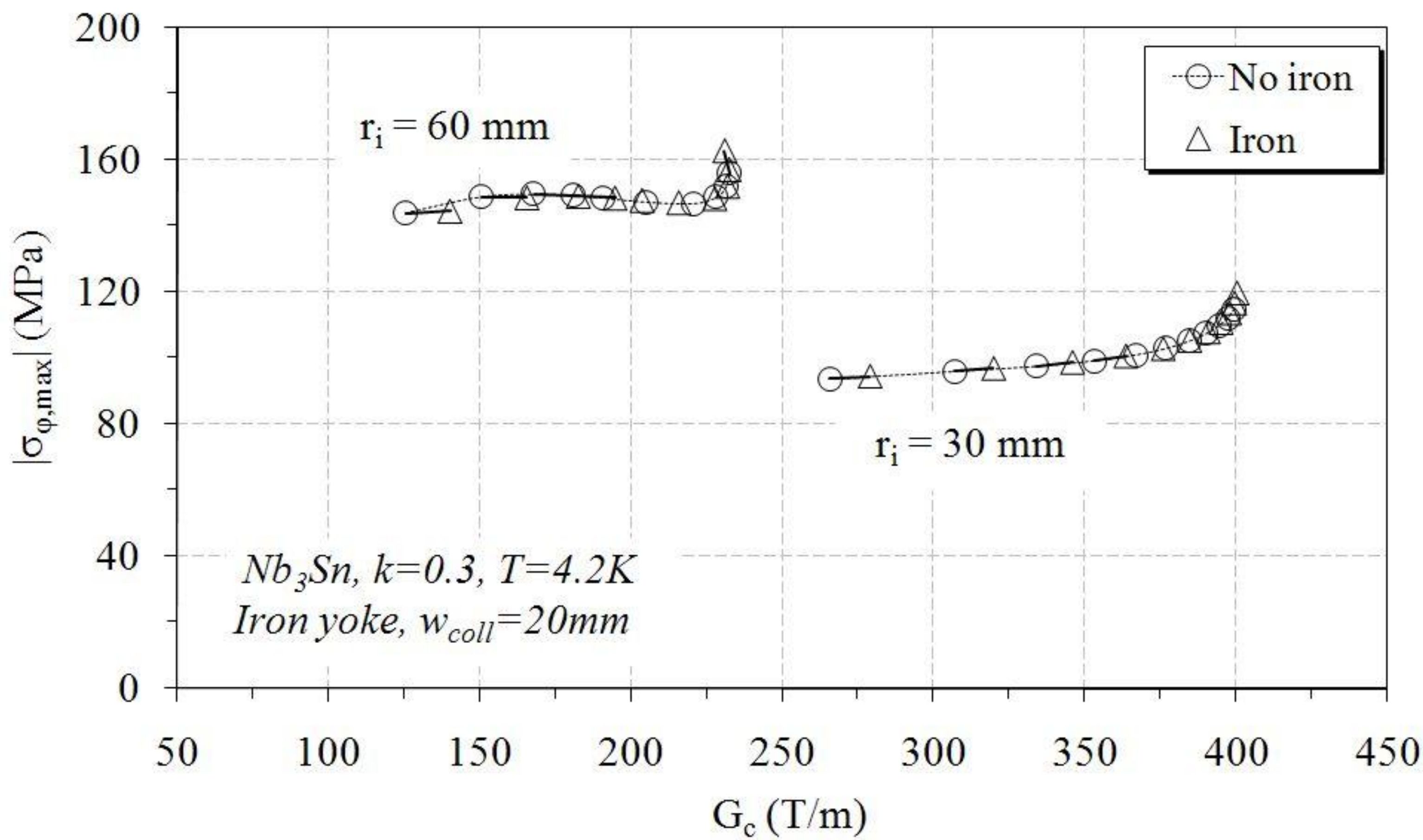

- The iron acts as a larger coil width, but the stress-gradient relation remains essentially the same.

CONTENTS

QUADRUPOLES
COMPARISON WITH REAL X-SECTIONS

- Different state of the art Nb-Ti quadrupoles have been considered as a bench test for the analytical approximation.
- Both cases of coil in air and iron screened were studied at short sample.
- Reference F_{mag} computed in Roxie

- Comparison based on the equivalent coil width, leading to the same coil surface A:

$$w_{eq} = \left(\sqrt{1 + \frac{3A}{2\pi r_i^2}} - 1 \right) r_i$$

	r_i (mm)	w_{eq} (mm)	k	T (K)	R_s (mm)	w_{coll} (mm)
LHC-MQ	28	28.4	0.254	1.9	90	31
LHC-MQM	28	17	0.263	1.9	102	27
RHIC MQ-ARC	40	9.1	0.228	4.6	55	5
HERA MQ	37.4	18.2	0.273	4.4	80	24
ISR MQ	116	32.1	0.346	4.4	176	22
Tevatron MQ	44.59	15.4	*0.243*	*4.0*	*101*	*41*
LHC-MQXA	34.94	37.4	*0.352*	*1.9*	*92*	*12*
LHC-MQXB	35	26.7	*0.338*	*1.9*	*92*	*26*

QUADRUPOLES
COMPARISON WITH REAL X-SECTIONS

AIR	Fx (MN/m)	Fy (MN/m)	Fx,an (MN/m)	Fy,an (MN/m)	%Diff,Fx	%Diff,Fy
LHC-MQ	0.69	-1.22	0.63	-1.17	-8.9	-4.1
LHC-MQM	0.38	-0.73	0.34	-0.70	-10.2	-4.4
RHIC MQ-ARC	0.09	-0.21	0.08	-0.20	-8.5	-5.9
HERA MQ	0.30	-0.61	0.27	-0.58	-9.7	-4.6
ISR MQ	1.22	-2.53	0.93	-2.17	-23.4	-14.1
Tevatron MQ	*0.17*	*-0.35*	*0.15*	*-0.33*	*-9.7*	*-5.4*
LHC-MQXA	*1.10*	*-2.04*	*1.04*	*-1.93*	*-5.1*	*-5.2*
LHC-MQXB	*0.76*	*-1.49*	*0.72*	*-1.41*	*-5.4*	*-5.4*

IRON	Fx (MN/m)	Fy (MN/m)	Fx,an (MN/m)	Fy,an (MN/m)	%Diff,Fx	%Diff,Fy
LHC-MQ	0.537	-0.732	0.515	-0.731	-4.2	-0.1
LHC-MQM	0.309	-0.446	0.300	-0.436	-2.9	-2.3
RHIC MQ_ARC	0.099	-0.0842	0.092	-0.077	-6.7	-8.3
HERA MQ	0.148	-0.187	0.134	-0.180	-9.5	-3.8
ISR MQ	0.911	-0.838	0.754	-0.685	-17.2	-18.2
Tevatron MQ	*0.137*	*-0.209*	*0.121*	*-0.201*	*-11.4*	*-4.0*
LHC-MQXA	*1.635*	*-1.573*	*1.356*	*-1.343*	*-17.1*	*-14.6*
LHC-MQXB	*0.868*	*-1.13*	*0.704*	*-0.925*	*-18.9*	*-18.1*

CONTENTS

Quadrupoles - Conclusions

- A simple analytical approach is presented, based on a 30° sector coil to estimate the peak azimuthal stress on coil.
- The azimuthal peak stress at short sample shows a localized maximum; it appears that for larger coil widths the increased gradient copes with a reduced peak stress.
- In Nb-Ti coils, the peak stress is always below 100 MPa (possible insulation creep).
- In Nb_3Sn coils, the peak stress can be below the assumed limit of 150 MPa for aperture radii up to 60 mm.
- A correction of the critical current density is proposed, based on a semi-analytical approach.
- With an iron screen, both G_c and the peak stress increase to the same level as it would be for an ironless coil, producing the same gradient.
- **All the computations have been performed at short sample. A safety operating margin of 20% would lead to a the peak stress reduction of ~40%.**

CONTENTS

- Aim of the work
- Forces and Stress in Quadrupoles
  - …
- Forces and Stress in Dipoles
  - Analytical formulae for e.m. forces and comparison with FEM models
  - Analytical formulae for mechanical stress and comparison with FEM models
  - E.m. forces and mechanical stress at short sample
  - Iron effect
  - Comparison with real cross sections
  - Conclusions

DIPOLES – COIL MODELS

Analytical coil model

- Sector coil layout at 60 (cancel the sextupole coefficient in the field series expansion)
- Constant current density $j(r)=j$
- Aperture radius r_i
- Coil equivalent width w

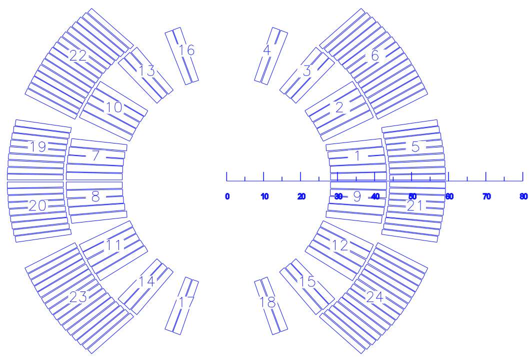

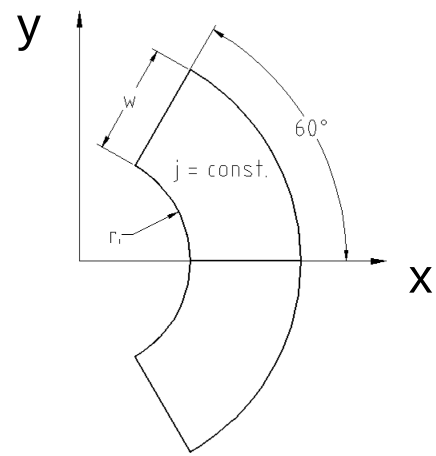

FEM coil model

- 2D FEM model - ANSYS™
- Coupled analysis: magnetic-mechanical
- Magnetic analysis solves for the Magnetic Vector Potential (A_z component)
- Mechanical symmetry constraints on coil mid-plain
- Infinitely rigid collar (radial mech. constraints)

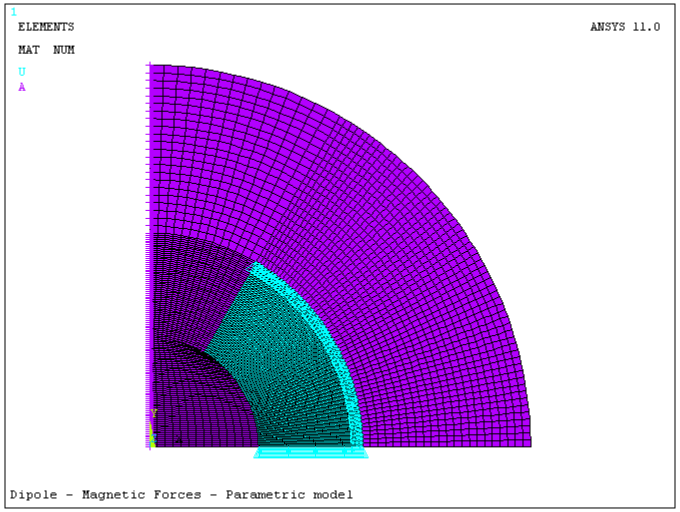

DIPOLES – ANALYTICAL MODEL VALIDATION
E.M. FORCES

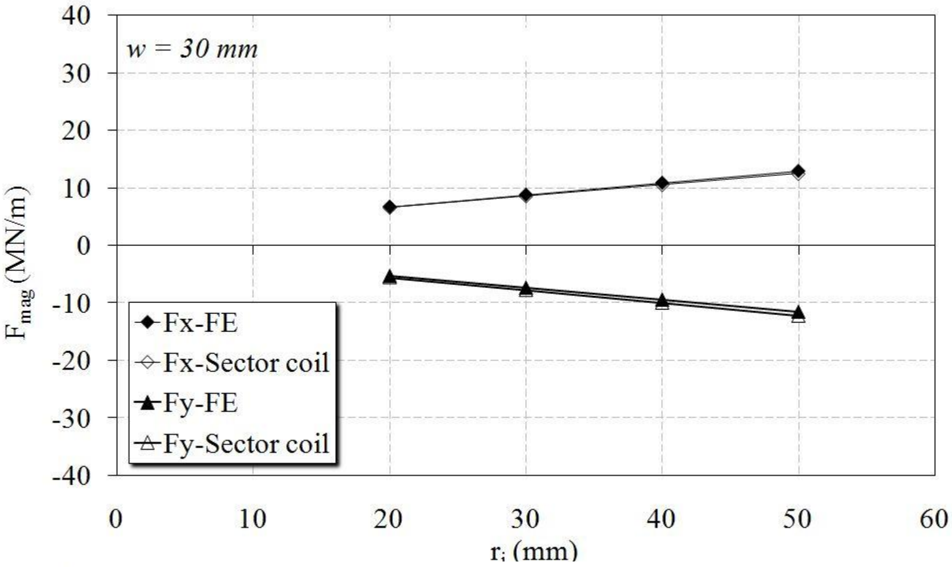

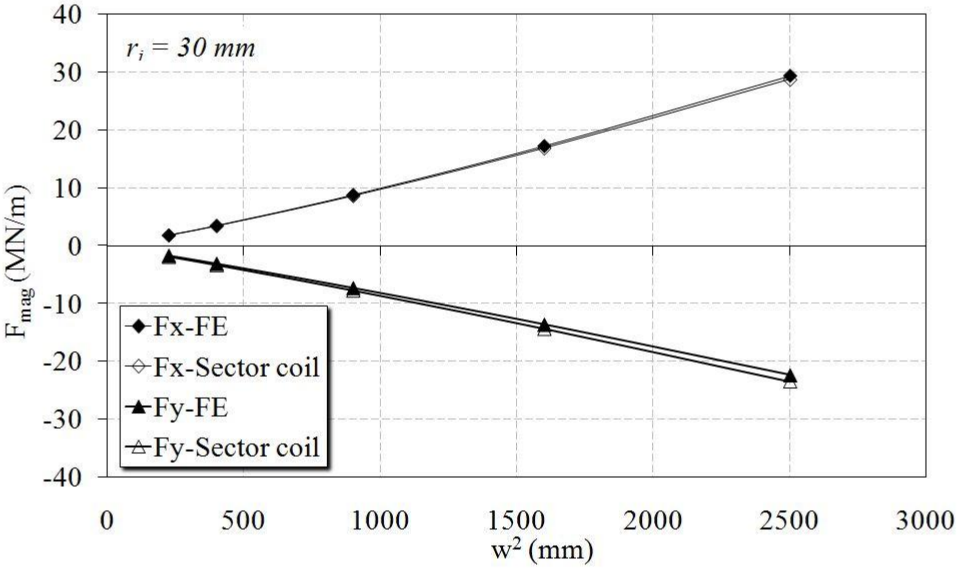

- Parametric analysis carried out on:
    1. r_i : [20, 30, 40, 50] mm
    2. w: [15, 20, 30, 40, 50] mm
- j=1000 A/mm^2 regardless of the layout

- The analytical approach does not well describe the magnetic field inside the coil
- On the other hand the magnetic energy and the magnetic forces are in good agreement with numerical results

- F_{mag} follow a linear trend with: r_i and w^2
- F_x underestimates the numerical value of about 3%
- F_y overestimates the numerical value of about 6%

Dipoles – Analytical model validation mechanical stress

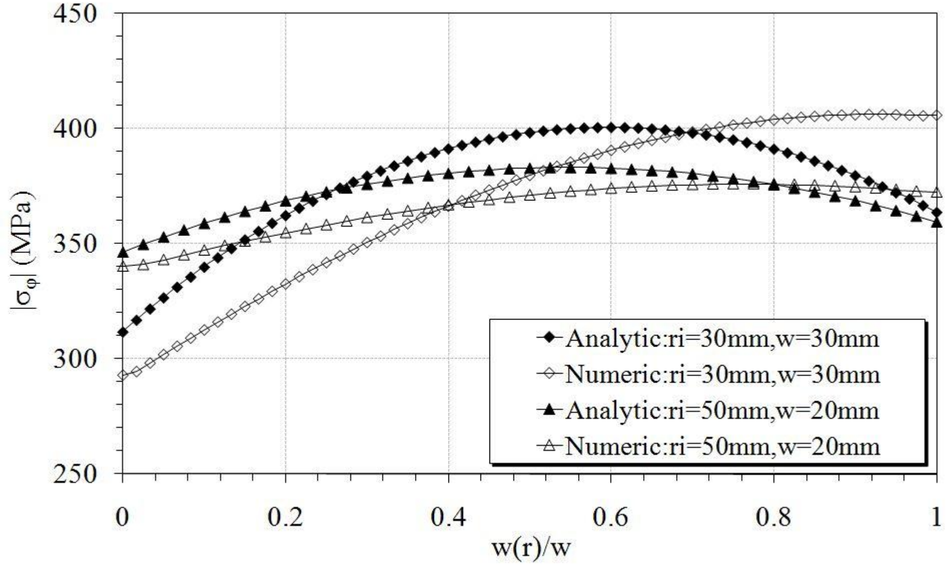

Azimuthal stress

$$\sigma_\varphi(r) = \frac{j^2 \mu_0 \sqrt{3}}{6\pi r} \left[r^3 + r_i^3 - 3r^2 (r_i + w) \right]$$

- Analytical approach: $\sigma_{\varphi,max}$ position is ~2/3 of coil width w
- Large aspect ratio w/r_i: $\sigma_{\varphi,max}$ position at the outer radius (numerical evidence)
- $\sigma_{\varphi,max}$ usually differs of 3% with the numerical value

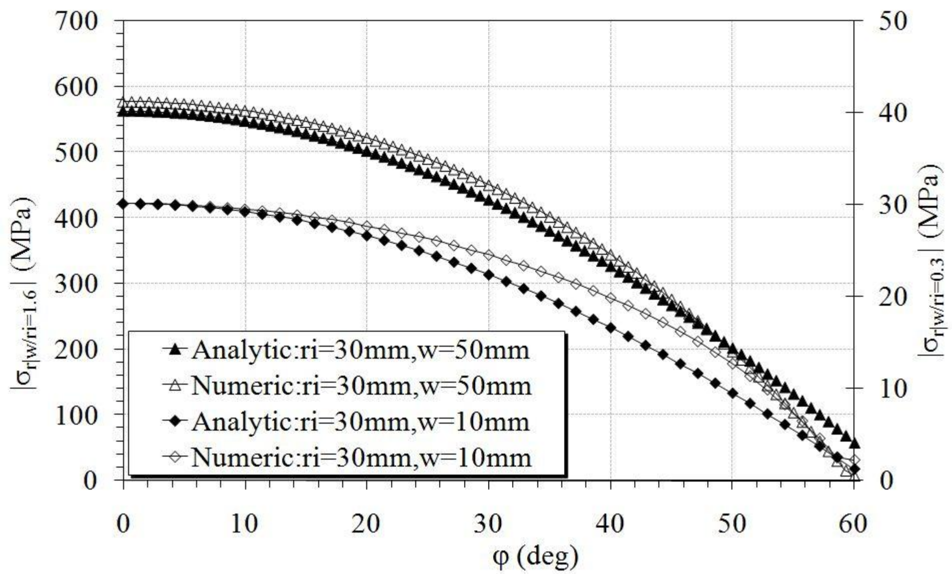

Radial stress

$$\sigma_r(\varphi) = \frac{j^2 \mu_0 \sqrt{3}}{18\pi (r_i + w)} f_{pr}\left(r_i^3, w^3, \varphi\right)$$

- $\sigma_{r,max}$ along the mid-plane (φ=0)
- The peak radial stress differs of ~1% with the numerical value

CONTENTS

Critical surface parameterization

Nb-Ti

$$j_{c,Nb-Ti} = \frac{\kappa c B_{c2}^{*}}{1 + \kappa c \lambda(r_i, w)\gamma_0 w}$$

Nb_3Sn

$$j_{c,Nb_3Sn} = \frac{\kappa c}{2}\left(\sqrt{\frac{4B_{c2}^{*}}{\kappa c \lambda \gamma} + 1} - 1\right)$$

- κ: cable dilution factor
  - $\kappa_{\text{Nb-Ti}}$ ranges in [0.23-0.3]
  - $\kappa_{\text{Nb}_3\text{Sn}}$ ranges in [0.26-0.48]
- B_{c2}: critical field (T)
- c: critical surface slope (A/Tm^2)
- $\lambda = B_p/B_0$ (adim)
- $\gamma = w\gamma_0 = w$6.93e-7 (60 layout) (Tm^2/A)

Central field $B_0 = j\gamma_0 w$

Peak field $B_p = j\lambda(r_i, w)\gamma_0 w$

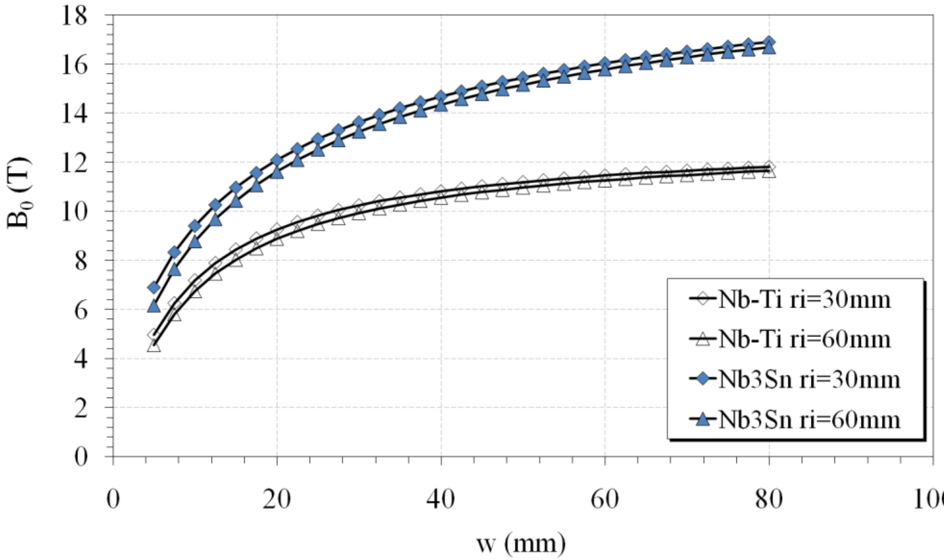

	Nb-Ti		Nb_3Sn	
T (K)	1.9	4.2	1.9	4.2
c (A/Tm^2)	6e8	6e8	4e9	3.9e9
B_{c2} (T)	13	10	23.1	21

L. Rossi, E. Todesco, "Electromagnetic design of superconducting dipoles based on sector coils", Phys. Rev. 10, 112401 (2007)

Dipoles – Forces at short sample

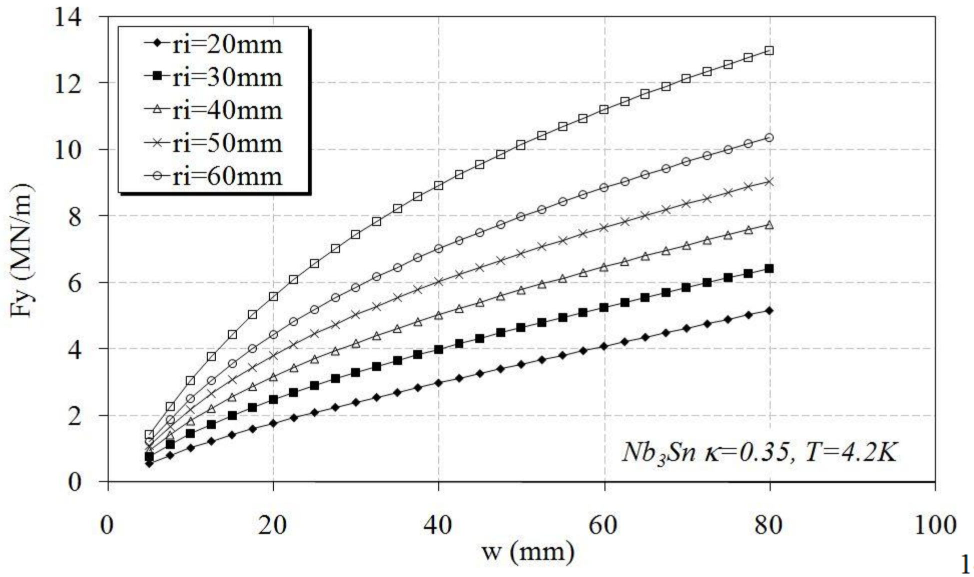

Model input

- κ set to 0.35 in order to have comparable results
- r_i ranges in [20-60] mm
- w ranges in [5-80] mm

- j increases of about 30-40% using Nb_3Sn instead of Nb-Ti, depending on the geometrical layout
- F_{mag} proportional to j^2
- *Small w*: higher central field matches higher forces for a cable add-on
- *Large w*: force trend tends to saturate together with B_0 for a cable add-on

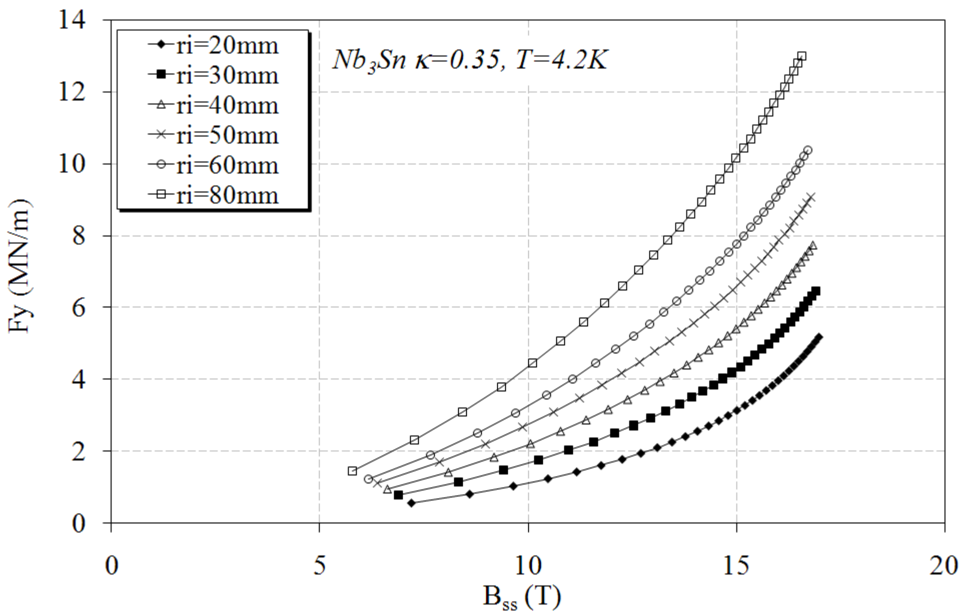

Dipoles – $\sigma_{\varphi,max}$ at short sample

$$\sigma_{\varphi,\max} = \frac{j^2 \mu_0 \sqrt{3}}{6\pi r} Max_{r \in [r_i, r_i+w]} \left[2r^3 + r_i^3 - 3r^2 (r_i + w) \right]$$

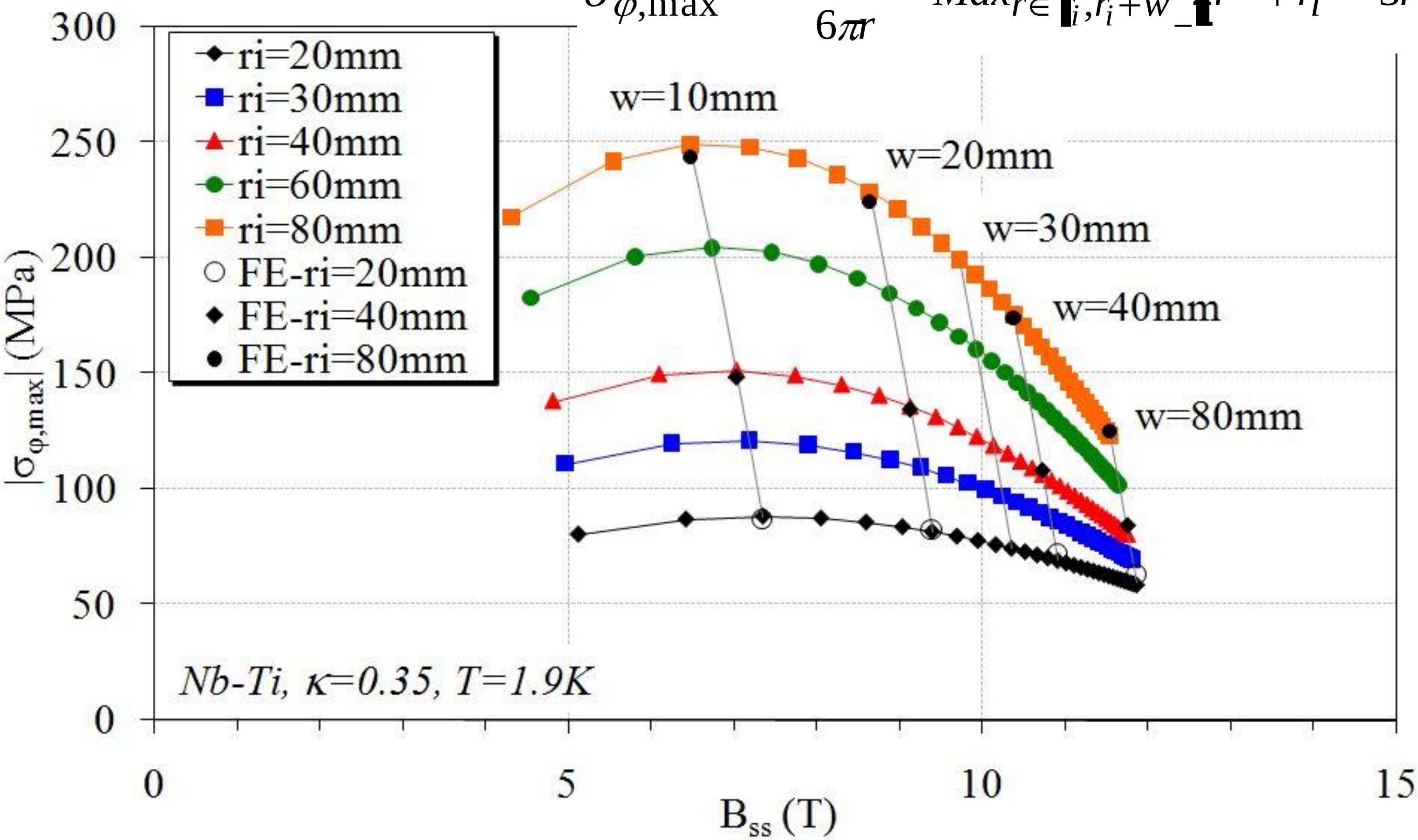

- Decrease in j^2 rules over the increase of the geometrical factor
- For larger coil width, higher field are achieved reducing at the same time the peak azimuthal stress.
- This effect increases for larger apertures

DIPOLES – $\sigma_{\varphi,max}$ AT SHORT SAMPLE

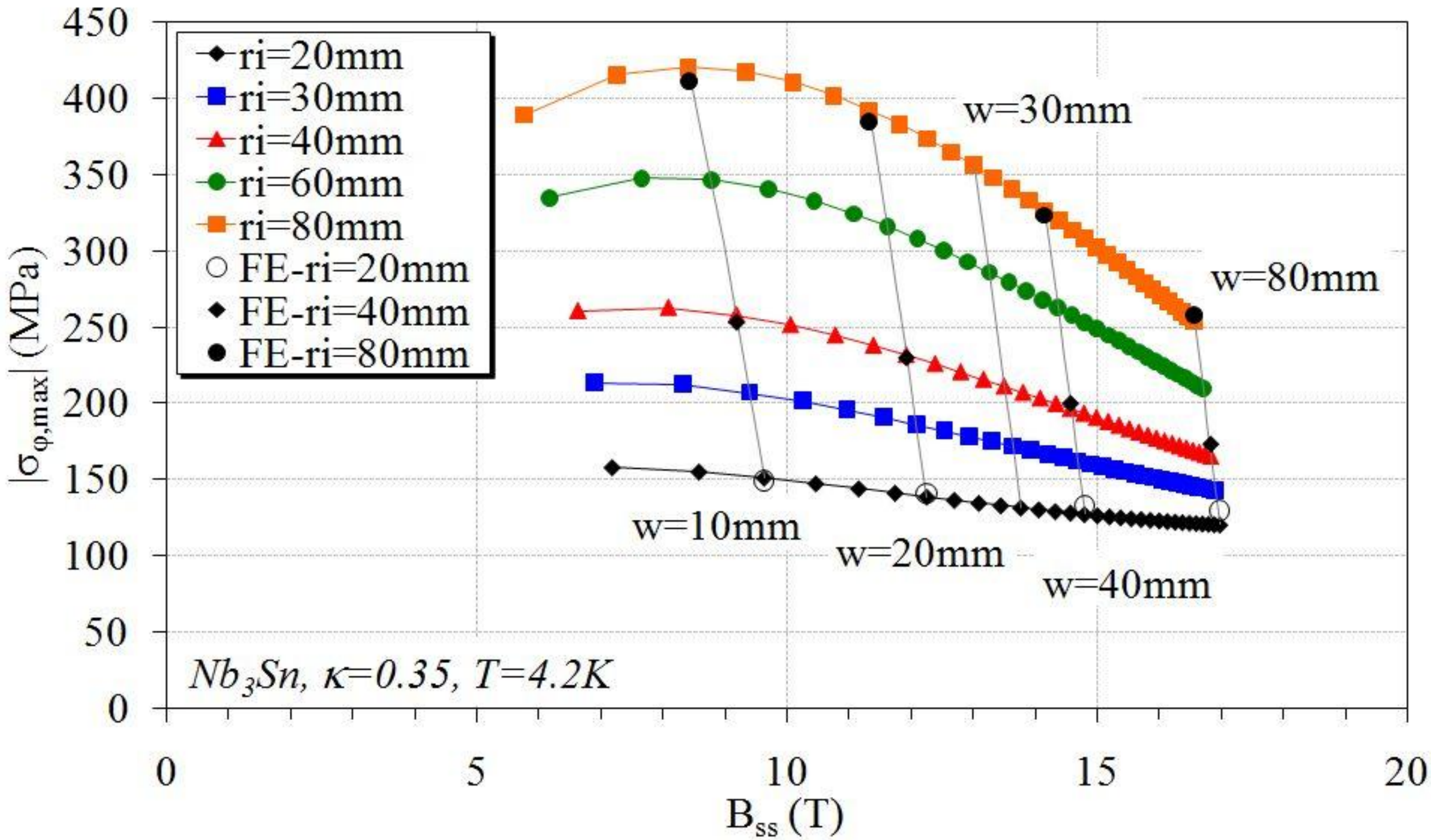

- For r_i<20 mm, the assumed limit of 150 MPa is not constraining the coil size.
- Less efficient but larger coil could bring the peak stress down (cost issue)
- r_i=30 mm, and B_0=15 T: κ=0.25 leads to $\sigma_{\varphi,max}$=130 MPa, but w=60 mm is required

DIPOLES – $\sigma_{\varphi,max}$ AT SHORT SAMPLE

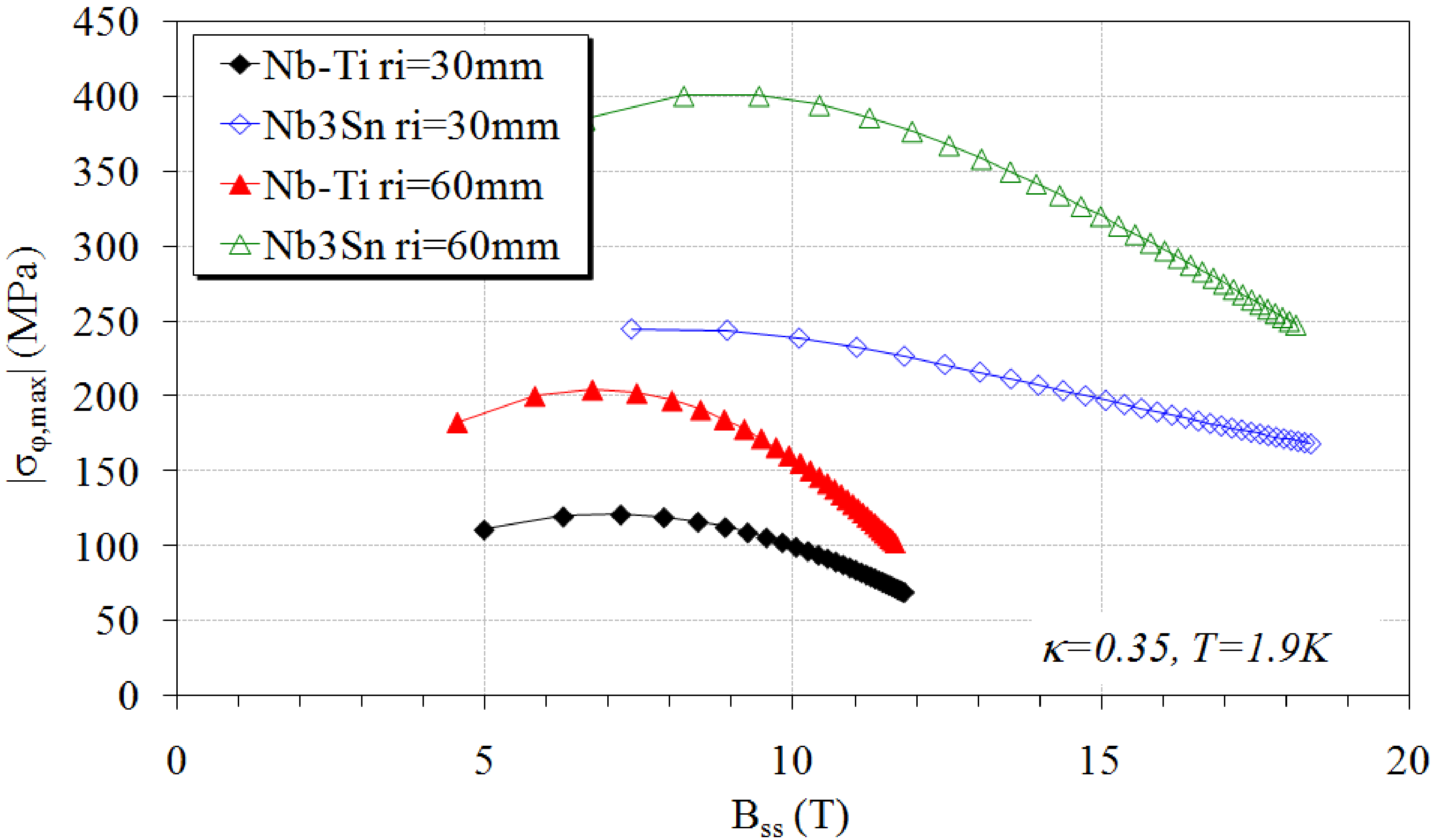

- T=1.9 K, $j_{c,Nb3Sn}/j_{c,Nb\text{-}Ti}$=1.5 → $\sigma_{\varphi,max(Nb3Sn)}=2.2\sigma_{\varphi,max(Nb\text{-}Ti)}$
- B_0=12 T (r_i=30 mm): $w_{Nb\text{-}Ti}$ = 80 mm (1.9K), w_{Nb3Sn}=20 mm (4.2K) →σ limited

CONTENTS

- Aim of the work
- Forces and Stress in Quadrupoles
  - …
- Forces and Stress in Dipoles
  - Analytical formulae for e.m. forces and comparison with FEM models
  - Analytical formulae for mechanical stress and comparison with FEM models
  - E.m. forces and mechanical stress at short sample
  - Iron effect
  - Comparison with real cross sections
  - Conclusions

Dipoles – Iron Effect

- Using an iron yoke we increase the bore field ΔB_0 and the peak field ΔB_p for a given j
- <u>The expression of j has to be revised</u>
- We do not account for field saturation
- B_0 and B_p are then considered as linear function of j

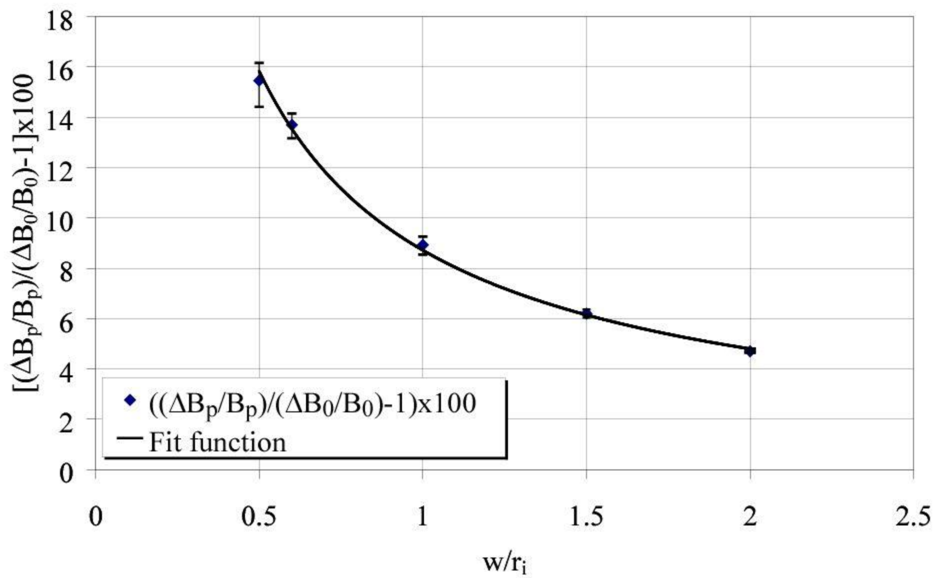

- The iron effect has been analytically accounted for using the *Image Current* approach
- Collar width: $w_{coll} = R_{yoke} - r_o$
- w_{coll} ranges in [10-60] mm, steps of 10 mm
- B_0 analytically derived
- B_p numerically evaluated

Empirical fit

$$\frac{\Delta B_p}{B_p} - \frac{\Delta B_0}{B_0} = \frac{\Delta B_0}{B_0}\left[p\left(\frac{w}{r_i}\right)^{-q}\right]$$

With:

- p=8.72e-2
- q=0.861

$\gamma_{iron} \rightarrow j_{iron}$

Dipoles – Iron effect

$$\sigma_{\varphi,\max} = \frac{j^2 r \mu_0 \sqrt{3}}{6\pi} Max_{r \in [r_i, r_i+w]} \left[2r - 3r_o + \frac{r_i^3}{r^2} - \left(\frac{\mu_r - 1}{\mu_r + 1} \right) \frac{r_o^3 - r_i^3}{R_{yoke}^2} \right]$$

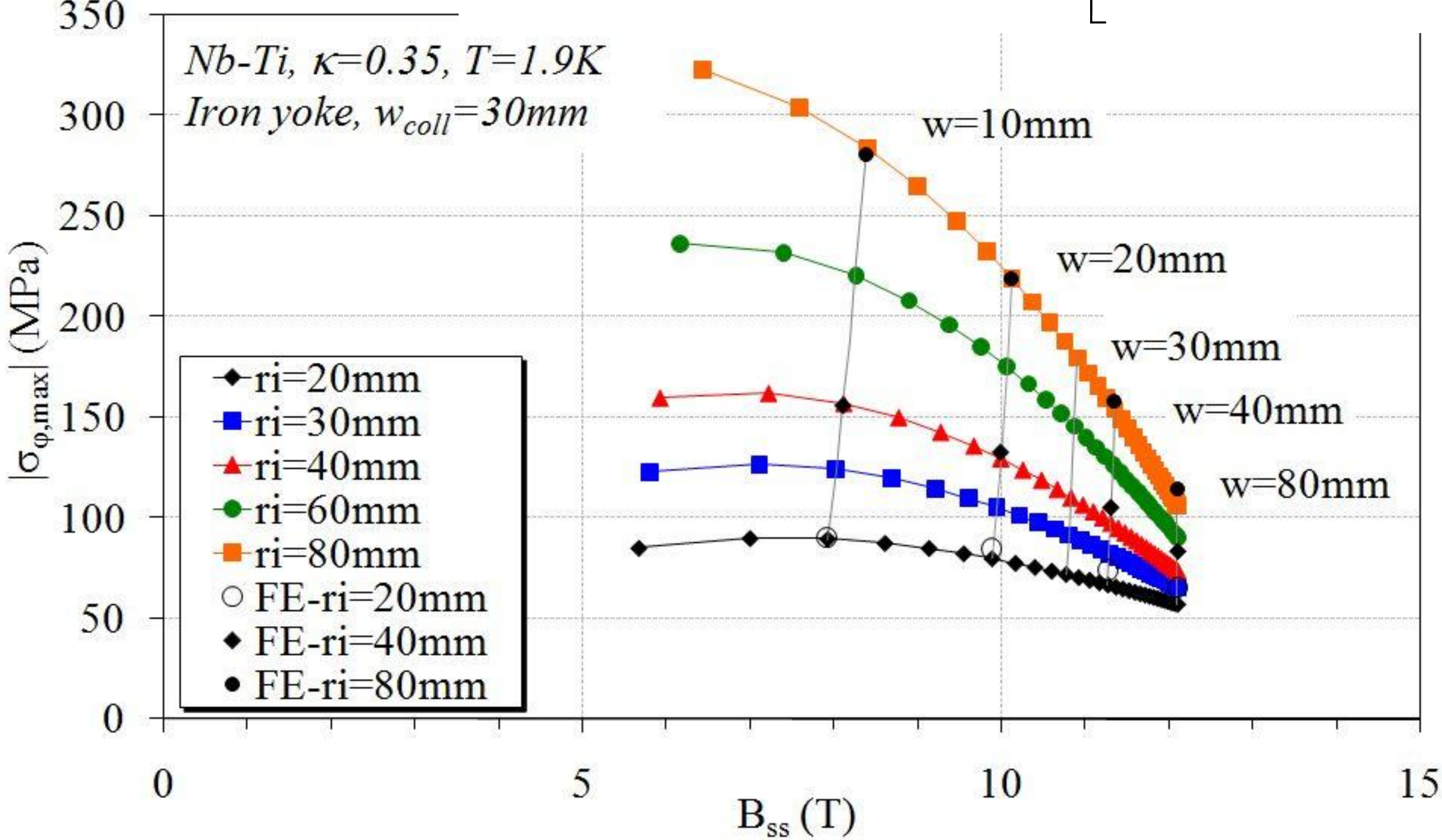

Max stress position

$$r\left(\sigma_{\varphi,\max}\right)_{iron} = a r_i + b w + c$$

- With: a=1.03, b=0.88, c=-2.96 mm

$$r_i \in [0-60]\,mm,\ w \in [0-50]\,mm,\ w_{coll} \in [20-35]\,mm$$

Dipoles – iron effect

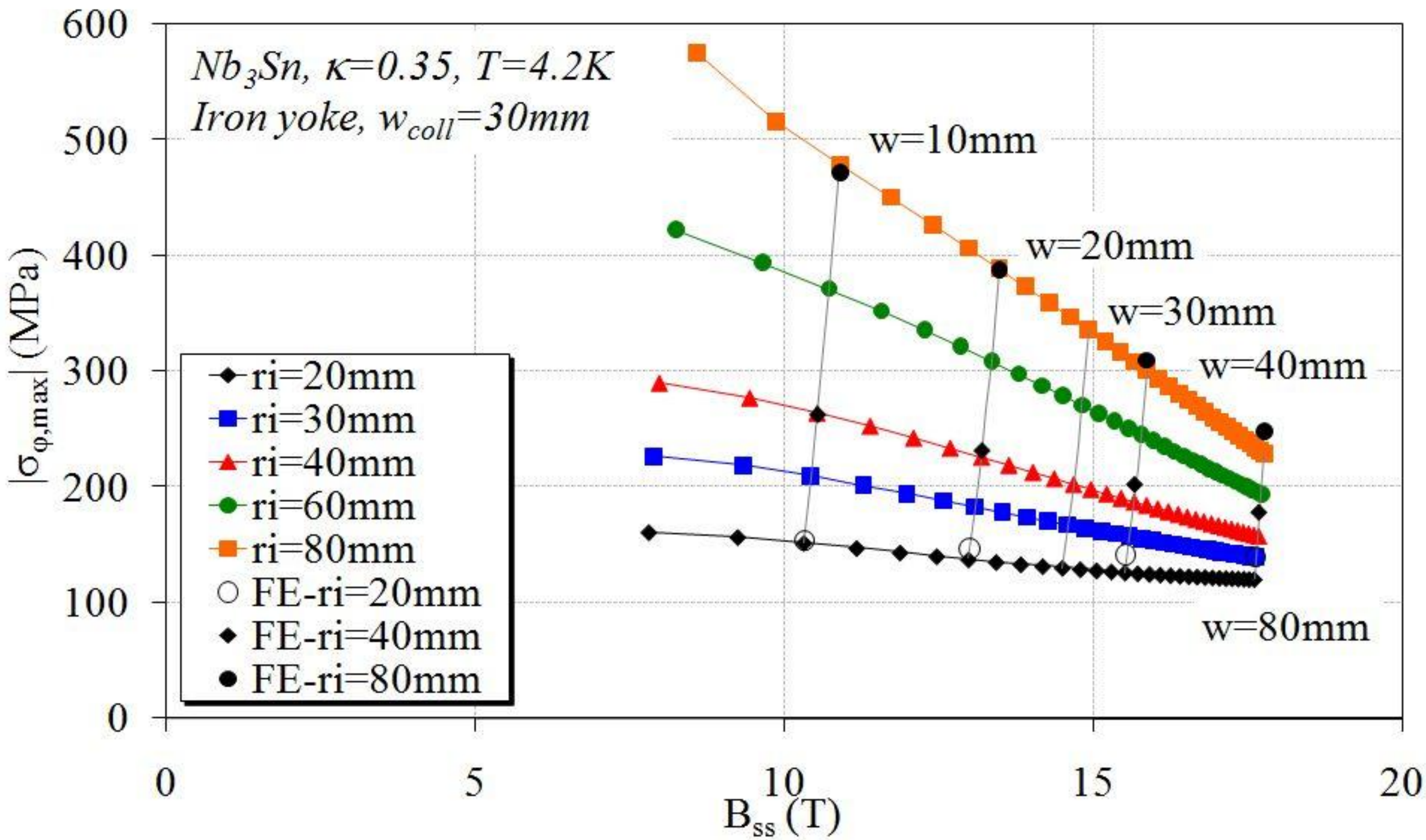

- The use of the iron yoke allows to: increase the bore field, reduce the current density j_{iron} as well as the peak stress on coil for a given layout (κ dependent).
- For a given B_0, a smaller width can be used, facing a slightly higher peak stress (few percent).

CONTENTS

- Aim of the work
- Forces and Stress in Quadrupoles
  - …
- Forces and Stress in Dipoles
  - Analytical formulae for e.m. forces and comparison with FEM models
  - Analytical formulae for mechanical stress and comparison with FEM models
  - E.m. forces and mechanical stress at short sample
  - Iron effect
  - Comparison with real cross sections
  - Conclusions

Dipoles – Comparison with real X-sections

- Different state of the art Nb-Ti dipoles have been considered as a bench test for the analytical approximation.
- Both cases of coil in air and iron screened were studied at short sample.

- Comparison based on the equivalent coil width, leading to the same coil surface A:

$$w_{eq} = \left(\sqrt{1 + \frac{3A}{2\pi r_i^2}} - 1 \right) r_i$$

	r_i (mm)	w_{eq} (mm)	w_{coll} (mm)	σ_φ,FE (MPa)	σ_φ,An (MPa)	%Diff.
RHIC MB	40.00	9.22	9.6	62.6	68.8	10
LHC MB	28.00	26.84	39.2	87.5	85.3	-3
SSC MB	25.00	21.52	19.4	53.3	49.8	-7
Tevatron MB	38.05	14.30	36.1	87.6	64.2	**-27**
HERA MB	37.50	18.74	28.2	87.0	62.1	**-29**

DIPOLES – COMPARISON WITH REAL X-SECTIONS

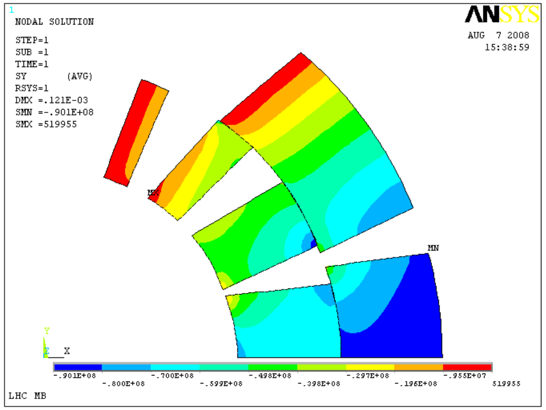

LHC-MB comparison

Cross section ←

Equivalent model →

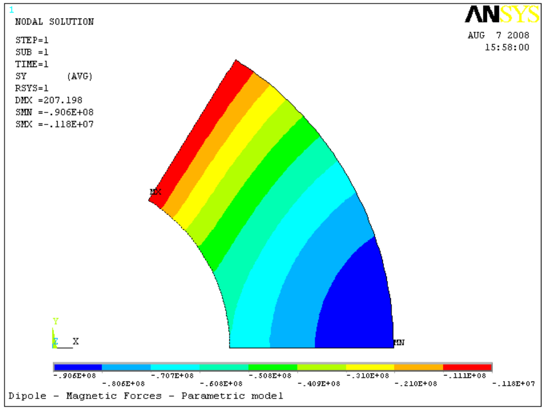

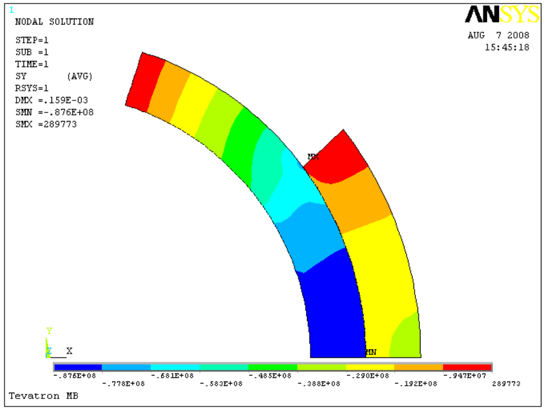

Tevatron-MB comparison

Cross section ←

Equivalent model →

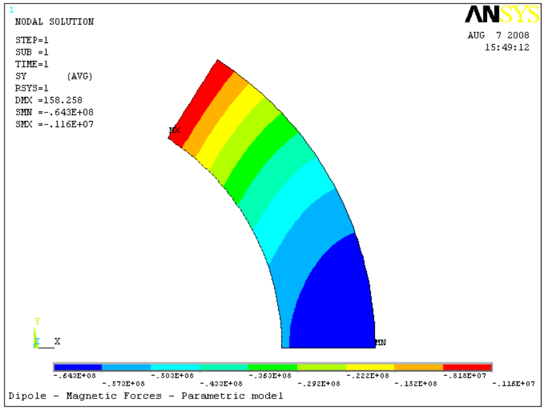

- The difference in forces is <10% along the X-Y Cartesian directions.
- Difference in peak stress is <10%, except for Tevatron MB and HERA MB where $\sigma_{\varphi,max}$ is <30% underestimated by the analytical approach.
- This effects depends on the augmented Δα angle between inner and outer layers: the higher Δα, the higher the peak stress, up to ~40% (test at 1000 A/mm^2).

CONTENTS

- Aim of the work
- Forces and Stress in Quadrupoles
  - …
- Forces and Stress in Dipoles
  - Analytical formulae for e.m. forces and comparison with FEM models
  - Analytical formulae for mechanical stress and comparison with FEM models
  - E.m. forces and mechanical stress at short sample
  - Iron effect
  - Comparison with real cross sections
  - Conclusions

DIPOLES – CONCLUSIONS

- A simple analytical approach is presented, based on a 60 sector coil to estimate the peak azimuthal stress on coil .
- The peak stress has been related to the coil geometrical layout and to the superconductor type.
- For aperture larger than 30 mm, larger and larger coils provide higher field and lower peak stress.
- For Nb_3Sn coils, aperture radii <30 mm feature $\sigma_{\varphi,max}$< 150 Mpa at short sample, regardless of the coil width.
- The use of an iron screen helps to reduce the coil width for a given B_0 and aperture, implying a slightly higher stress.
- A comparison with some dipoles cross sections reveals agreement between numerical and analytical results <30%. This agreement is reduced to 10% for coils whose aspect ratio is closer to 60 sector coil (effect of the relative angle Δα).
- **All the computations have been performed at short sample. A safety operating margin of 20% would lead to a the peak stress reduction of ~40%.**
- A further reduction of the peak stress could be also achieved by designing a less effective coil, eventually increasing the number of winding turns (manufacturing and cost issue).